NRC Publications Archive
Archives des publications du CNRC

Controlling n-heptane HCCI combustion with partial reforming : Experimental results and modeling analysis

Hosseini, Vahid; Neill, W. Stuart; Checkel, M. David

NRC Publications Record / Notice d'Archives des publications de CNRC:
https://nrc-publications.canada.ca/eng/view/object/?id=1964efdf-edd6-4ae4-9f51-44cb4bce6d7e
https://publications-cnrc.canada.ca/fra/voir/objet/?id=1964efdf-edd6-4ae4-9f51-44cb4bce6d7e

National Research Council Canada   Conseil national de recherches Canada

Canada

Controlling *n*-Heptane HCCI Combustion With Partial Reforming: Experimental Results and Modeling Analysis

Vahid Hosseini

W. Stuart Neill

Institute for Chemical Process and
Environmental Technology,
National Research Council,
Ottawa, ON, K1A 0R6, Canada

M. David Checkel
University of Alberta,
Edmonton, AB, T6G 2G8, Canada

One potential method for controlling the combustion phasing of a homogeneous charge compression ignition (HCCI) engine is to vary the fuel chemistry using two fuels with different auto-ignition characteristics. Although a dual-fuel engine concept is technically feasible with current engine management and fuel delivery system technologies, this is not generally seen as a practical solution due to the necessity of supplying and storing two fuels. Onboard partial reforming of a hydrocarbon fuel is seen to be a more attractive way of realizing a dual-fuel concept, while relying on only one fuel supply infrastructure. Reformer gas (RG) is a mixture of light gases dominated by hydrogen and carbon monoxide that can be produced from any hydrocarbon fuel using an onboard fuel processor. RG has a high resistance to auto-ignition and wide flammability limits. The ratio of H_2 to CO produced depends on the reforming method and conditions, as well as the hydrocarbon fuel. In this study, a cooperative fuel research engine was operated in HCCI mode at elevated intake air temperatures and pressures. n-heptane was used as the hydrocarbon blending component because of its high cetane number and well-known fuel chemistry. RG was used as the low cetane blending component to retard the combustion phasing. Other influential parameters, such as air/fuel ratio, EGR, and intake temperature, were maintained constant. The experimental results show that increasing the RG fraction retards the combustion phasing to a more optimized value causing indicated power and fuel conversion efficiency to increase. RG reduced the first stage of heat release, extended the negative temperature coefficient delay period, and retarded the main stage of combustion. Two extreme cases of RG composition with H_2/CO ratios of 3/1 and 1/1 were investigated. The results show that both RG compositions retard the combustion phasing, but that the higher hydrogen fraction RG is more effective. A single-zone model with detailed chemical kinetics was used to interpret the experimental results. The effect of RG on combustion phasing retardation was confirmed. It was found that the low temperature heat release was inhibited by a reduction in intermediate radical mole fractions during low temperature reactions and during the early stages of the negative temperature coefficient delay period. [DOI: 10.1115/1.3078189]

1 Introduction

Diesel engine manufacturers are pursuing a variety of combustion strategies for simultaneously achieving high fuel conversion efficiency while producing near-zero engine-out NO_x and particulate matter (PM) emissions, which is commonly referred to as high efficiency clean combustion (HECC). The mixing-controlled HECC strategy involves the use of higher levels of exhaust gas recirculation (EGR) than current diesel technology to reduce the combustion temperatures. This technology appears to require very high fuel injection pressures with small injector nozzle holes and benefits from the use of an oxygenated diesel fuel (see Ref. [1]). The premixed HECC or HCCI strategy involves the uncontrolled auto-ignition of a homogeneous air/fuel mixture under highly diluted conditions with excess air and/or EGR. It has been shown to produce very low NO_x and PM emissions and has the potential to have a high fuel conversion efficiency due to the short duration of heat release. On the other hand, HCCI combustion suffers from the lack of a direct method to control combustion phasing, as well as high HC and CO emissions [2].

HCCI combustion phasing may be controlled indirectly by varying the in-cylinder temperature history or by altering the auto-ignition properties of the fuel chemistry. Parameters that affect the in-cylinder temperatures include the intake temperature, intake pressure, compression ratio, engine speed, and coolant temperature. The fuel composition directly affects the auto-ignition process, which is commonly specified in terms of cetane number for diesel fuel or octane number (resistance to auto-ignition) for gasoline. Other parameters, such as relative air/fuel ratio (λ), residuals, and EGR affect both the in-cylinder temperatures and chemical composition.

The dual-fuel approach to altering diesel fuel chemistry by blending an appropriate quantity of a secondary fuel with a higher resistance to auto-ignition is one way to control the combustion phasing over a wide operating range independent of engine load. Several previous studies have examined dual-fueled HCCI combustion. Christensen et al. [3] examined a single-cylinder engine in HCCI mode with various blends of *n*-heptane/iso-octane and regular gasoline/diesel blends. In an experimental study by Stanglmaier et al. [4], fuel blending of additized F-T naphtha and natural gas was effectively used to control the phasing of HCCI combustion. Zheng et al. [5] examined dual-fuel HCCI combustion using dimethyl ether (DME)/methanol blends to expand the operating range.

Dual-fuel engines are not desirable due to the necessity of car-
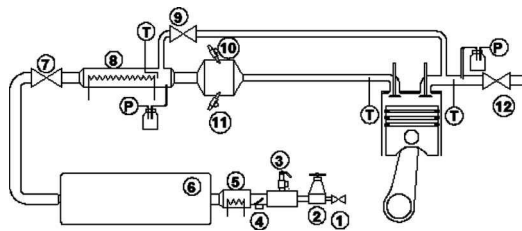
Copyright © 2009 by ASME

Fig. 1 Schematic of the CFR engine experimental setup, described in Table 1

rying two fuels onboard. Instead, partial reforming of diesel fuel with an onboard fuel reformer, which produces hydrogen rich gases, as the secondary fuel seems to be an attractive solution. This paper explores the possibility of HCCI combustion phasing control of a diesel-type fuel using reformer gas (RG).

RG or synthetic gas (syngas) is a mixture of light gases dominated by H_2 and CO. Steam reforming of natural gas is the main industrial method to produce H_2 in large quantities. Fuel reforming can be done by partial oxidation, steam reforming, or autothermal conversion. Details of reforming principles and techniques may be found in previous literature such as Ref. [6] or Ref. [7].

Shudo [8] altered the HCCI combustion of DME by adding H_2 and CO. The effect of RG on HCCI combustion of natural gas was investigated by Tsolakis and Megaritis [9]. It was found that the combustion phasing and duration were significantly changed by RG addition, leading to reductions in NO_x and PM emissions using diesel and biodiesel fuels. Eng et al. [10] studied the effects of partial oxidation RG on HCCI combustion of iso-octane and *n*-heptane. The authors also investigated the detailed chemical kinetics of H_2 enrichment on iso-octane and *n*-heptane autoignition. Hosseini and Checkel [11–13] investigated the effects of RG addition on HCCI combustion of a series of low octane primary reference fuels (PRFs), high octane PRFs, and natural gas.

2 Experimental Setup

A single-cylinder cooperative fuel research (CFR) engine manufactured by Waukesha Engine was used for the experiments. The engine has a variable compression ratio, a pancake combustion chamber with flat-top piston, and a bore $\times$ stroke of 82.6×114.3 mm^2. Compressed air was used to supply air to the engine. An electrical heater (8) was installed inside the intake to control the air temperature. Recirculated exhaust gas (EGR) was controlled manually by adjusting a manual EGR gate valve (9) as well as a butterfly valve (12) to set the exhaust back pressure. Liquid (10) and gaseous (11) injectors were installed in the intake plenum to fuel the engine. Figure 1 shows the main experimental hardware. The component description is provided in Table 1.

Table 1 List of the main components of the experimental setup in Fig. 1

Item No.	Description
1	Air supply main valve
2	Intake pressure regulator
3	High pressure relief valve
4	Low pressure relief valve
5	Hot wire anemometer
6	Intake pulsation damping barrel
7	Throttle valve
8	Intake heater
9	EGR valve
10	*n*-heptane injector
11	RG injector
12	Exhaust back-pressure valve

3 Operating Conditions

The engine was operated under steady state conditions with a constant speed of 800 rpm. The compression ratio was fixed at 11.8. The intake temperature of the air, fuel, RG, and EGR mixture just prior to entering the engine, $T_{intake,mix}$, was maintained at 110°C. Intake absolute pressure was kept constant at 140 kPa. The *n*-heptane mass flow rate was decreased as the RG blend fraction increased to maintain a constant air/fuel ratio. For example, if the engine was operated at 800 rpm, wide open throttle, atmospheric intake pressure, and λ=2.0, increasing RG blend fraction from 0% to 30% corresponded to a 23% decrease in the *n*-heptane mass flow rate. Since liquid fuel was being replaced with gaseous fuel, the air mass flow rate to the engine was reduced by 3%, and the total energy flow rate to the engine was reduced by 1%. Hence, RG was introduced to the intake mixture as "RG blending" and not "RG enriching."

4 Definitions

EGR was defined as the ratio of CO_2 concentration in the intake to CO_2 concentration in the exhaust. RG blending as defined on a mass basis as RG blend fraction=$100 \times \dot{m}_{RG}/(\dot{m}_{RG}+\dot{m}_{n\text{-heptane}})$, where $\dot{m}$ is the mass flow rate of *n*-heptane or RG.

Relative air/fuel ratio was calculated using the chemical valence method as described in [14] due to the presence of oxygen (CO) in the reformer gas. A more comprehensive method for calculating the air/fuel ratio of oxygenated fuels (or when oxidizer contains fuel) was described by Mueller [15].

Heat release calculations were performed using a single-zone well-stirred model using air as the working fluid, as described in Ref. [16]. The Woscnhi heat transfer correlation for HCCI engines [17] was used to calculate gross heat release (GHR) from net heat release. Referring to the net rate of heat release (NRHR) graph in Fig. 2(*a*), the maximum low temperature net rate of heat release (LTHR$_{max}$), maximum high temperature net rate of heat release (HTHR$_{max}$), and negative temperature coefficient (NTC) duration are defined. Using the cumulative gross heat release graph in Fig. 2(*b*), the start of combustion (SOC) is defined as the crank angle degree (CAD), where 10% of GHR$_{max}$ occurs and combustion duration (CD) was defined as the time it requires to go from SOC to 90% of GHR$_{max}$ on a CAD basis.

An uncertainty analysis was performed to quantify the cyclic variations of key combustion parameters. The key combustion parameters (SOC, CD, LTHR$_{max}$, HTHR$_{max}$, NTC, and indicated mean effective pressure (IMEP)) were calculated for 100 individual engine cycles and were averaged. In this paper, the error bars that appear in the graphs represent $\pm 2\sigma$.

5 Fuels

n-heptane was selected for this study because it is a volatile diesel fuel component with a high cetane number (54). It was injected into the intake plenum at a low pressure (413 kPa). The high volatility of *n*-heptane and the elevated intake temperature ensured that complete fuel vaporization occurred even at low port fuel injection pressures.

Simulated RG was provided from a high pressure tank. A natural gas injector supplied by alternative fuel systems was used. The injection pressure was held constant at 689 kPa. Two simulated RG compositions were examined. RG 75/25 was a mixture of 75% H_2−25% CO, and RG 50/50 was a mixture of 50% H_2−50% CO by volume. RG 75/25 was representative of a high H_2 content RG (to intensify H_2 effects) that is produced by steam reforming of natural gas. Onboard reforming of gasoline or diesel fuels produces RG similar to RG 50/50 through partial oxidation or autothermal reforming. The two RG cases of 75/25 and RG 50/50 represent the high and low limits for H_2 content, respectively. A comparison of the characteristics of RG 75/25 and RG 50/50 may be found in Ref. [18]. In practice, RG contains inert gases such as
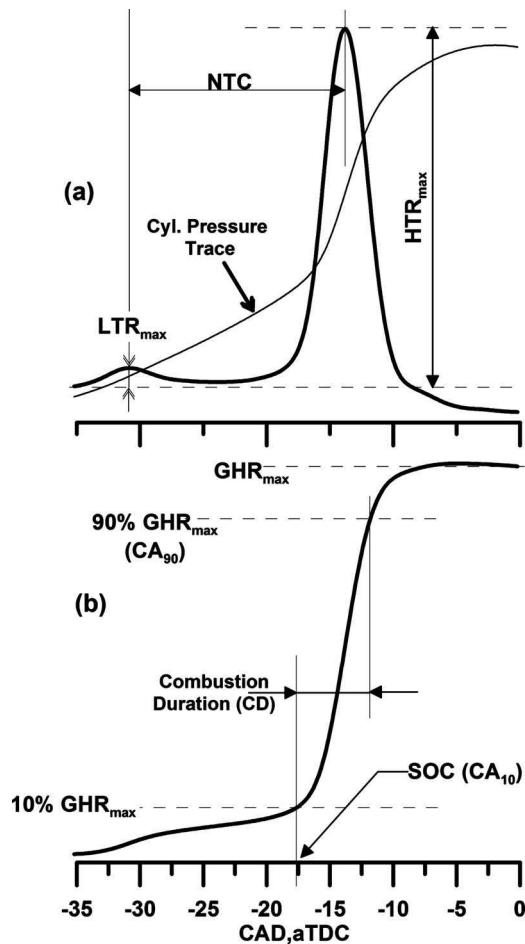
Fig. 2 Combustion characteristic definitions using (a) net rate of heat release and (b) gross cumulative heat release curves

Fig. 3 Selected λ-EGR constant cases, n-heptane HCCI combustion, $N=800$ rpm, CR=11.8, and $T_{intake,mix}=110°C$

control for the same operating region, which corresponds to an IMEP reduction of 1.8 bar (see Ref. [19] for baseline experiments).

Figure 6 shows that increasing the RG blend fraction did not significantly affect the combustion duration, which for the purposes of this study was defined as the number of crank angle degrees between 10% and 90% heat release. Since the RG blend fraction affects low temperature heat release (LTHR), which was

N_2, CO_2, and H_2O. A portion of the EGR may be considered to be the inert component of RG. For example, at $RG_{mass,frac}=10\%$ and a stoichiometric mixture for n-heptane HCCI combustion, 10% of fuel mass and less than 0.7% of intake mixture is occupied by RG. If it is assumed that RG is a product of partial oxidation with air, and 75% of RG mixture is made up of inert gases, the total amount of EGR that should be considered to be the inert gas part of RG is 0.5% of intake mixture. Hence, in this case 0.5% of EGR (as EGR is also quantified by percent intake mixture) is considered to be the inert gas fraction of RG.

6 Experimental Results

Operating points. A series of experiments were performed at constant λ and EGR conditions, as indicated in Fig. 3. Each group is labeled with capital letters A–F, and the symbols used in Fig. 3 remain unchanged throughout the paper. The majority of constant λ cases had high EGR rates, as the operating region was large enough to group a series of constant λ data. The variation between λ and EGR within each group is shown by an uncertainty value indicated by a ± sign. In each group, the RG blend fraction was progressively increased from 0% to 30%.

Heat release characteristics. Figure 4 shows the NRHR and gross cumulative heat release for data set B shown in Fig. 3.

Figure 5 shows that increasing the RG blend fraction effectively retarded n-heptane HCCI combustion timing, while keeping all other influential parameters constant. On average; a 10% increase in the RG blend fraction retarded the combustion phasing by 4.4 CAD for the cases considered. It would require an increase in λ of 0.88 to achieve a similar delay in the combustion phasing using λ
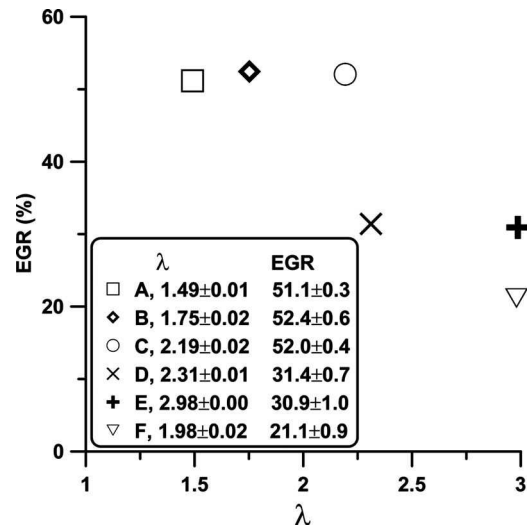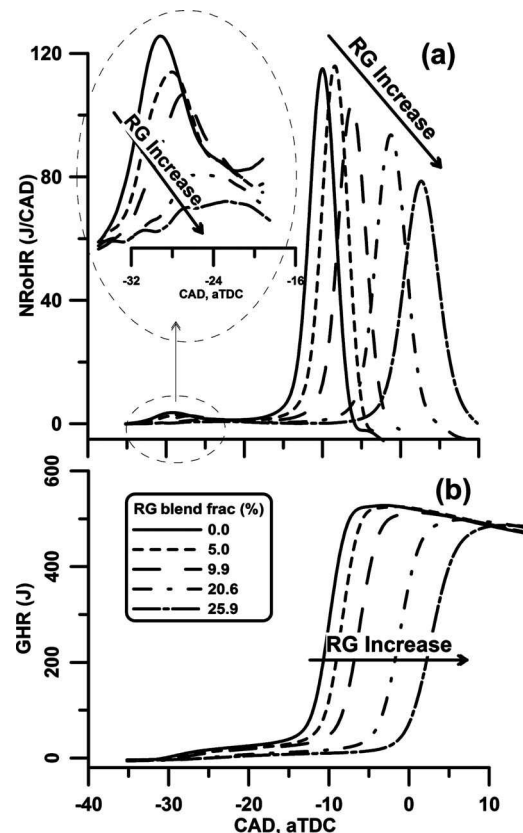

Fig. 4 Effect of RG on (a) net rate of heat release and (b) gross cumulative heat release for data set B in Fig. 3

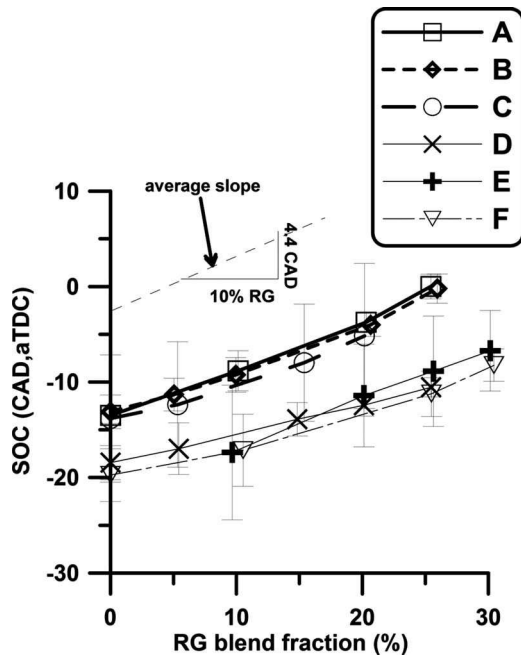Fig. 5 Effect of RG on start of combustion for operating points in Fig. 3, error bars indicate ±2σ

Fig. 7 Effect of RG on maximum low temperature heat release for operating points indicated in Fig. 3, error bars indicate ±2σ

typically less than 5% of the heat release, the RG did not change the duration of the high temperature heat release (HTHR) stage according to our definition.

Figure 7 shows the effect of RG on maximum low temperature rate of heat release (LTHR$_{max}$). Increasing the RG blend fraction by 10% decreased LTHR$_{max}$ by about 15%. The start of the LTHR stage remained relatively constant. The gross heat release was constant for all cases due to the constant energy flow to the engine (see Fig. 4(b)), while HTHR$_{max}$ was reduced due to the retardation of HTHR$_{max,time}$ (see Figs. 4(a) and 8).

Replacing n-heptane with RG was expected to reduce the heat capacity of the intake mixture and to increase the ratio of specific heats resulting in higher compression temperatures. As the start of the LTHR stage is highly temperature dependent, it was expected that the LTHR timing might be advanced due to higher compres-
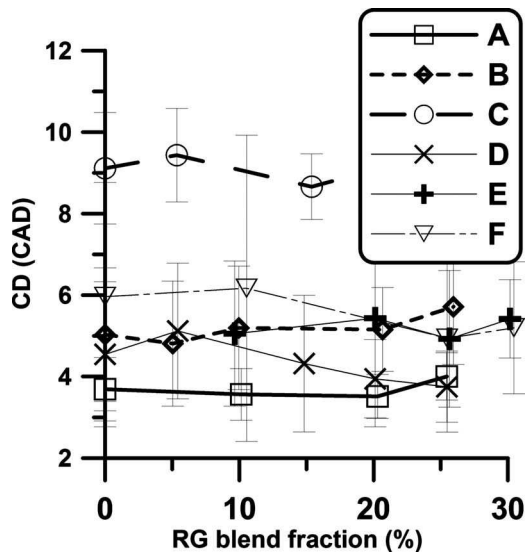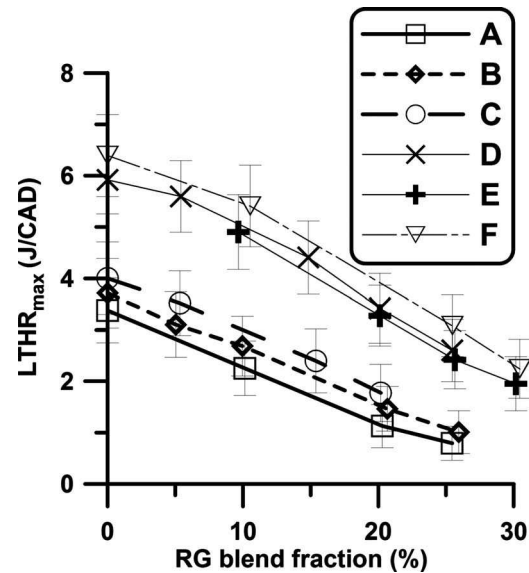
sion temperatures. However, the start of LTHR was not significantly affected by RG addition. LTHR heat release was relatively small compared with the HTHR heat release and it was difficult to detect the start of LTHR.

Thus, the timing of the LTHR stage was characterized by the location of peak heat release (LTHR$_{max}$). Increasing the RG blend fraction reduced LTHR$_{max}$ by suppressing the low temperature combustion reactions and consequently retarding LTHR$_{max,time}$. The gross cumulative heat release (Fig. 4(b)) remained constant, as energy flow to the engine was held constant. However, the HTHR$_{max,time}$ was retarded considerably by increasing the RG blend fraction. Figure 8 shows that HTHR$_{max,time}$ was retarded by approximately 5.1 CAD when the RG blend fraction was increased by 10%. This was slightly more than the 4.4 CAD delay in the SOC for 10% RG blending, which may be related to the

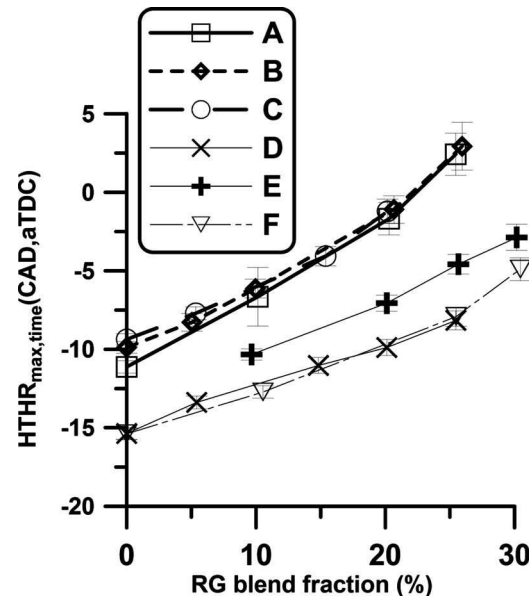Fig. 6 Effect of RG on combustion duration for operating points in Fig. 3, error bars indicate ±2σ

Fig. 8 Effect of RG on maximum high temperature heat release timing for operating points indicated in Fig. 3, error bars indicate ±2σ
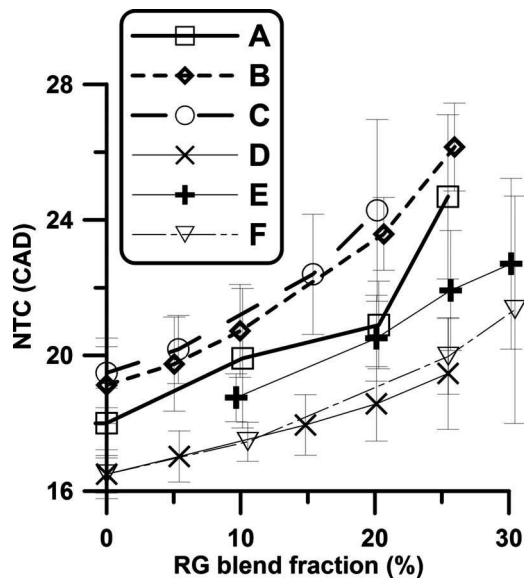
Fig. 9 Effect of RG on negative temperature coefficient duration for operating points indicated in Fig. 3, error bars indicate ±2σ

Fig. 11 Effect of RG on indicated thermal efficiency (η_{th}) for operating points in Fig. 3, error bars indicate ±2σ

slight retardation in $LTHR_{max,time}$. Increasing the RG blend fraction reduced $LTHR_{max}$, hence the required energy to initiate the main combustion stage had to be supplied by the compression process. Figure 9 shows that the NTC duration increases with increasing RG blend fraction due to a relatively constant $LTHR_{max,time}$ and a delayed $HTHR_{max,time}$.

Power and efficiency. Stable HCCI combustion was achieved as indicated by a coefficient of variation in IMEP of less than 3% for all operating points investigated. As the RG fraction was increased, IMEP increased due to the retardation of the combustion phasing toward an optimal combustion phasing. Figure 10 shows that a 10% increase in RG blend fraction led to an average IMEP increase of 0.25 bar due to the more optimized combustion phas-
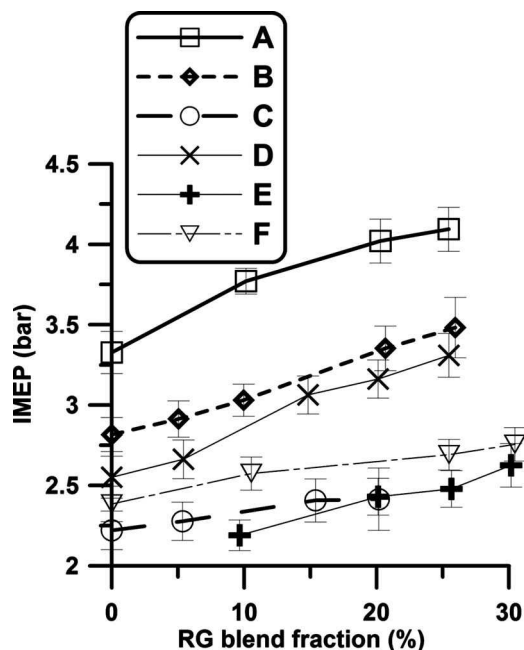
ing. This caused a 2.8% increase in thermal efficiency (η_{th}) on average for each 10% RG blend fraction increase, as indicated in Fig. 11.

The combustion timings for all cases examined in this study were advanced. The retardation of combustion timing by higher EGR, lower intake temperature, lower compression ratio, or higher λ was not possible.

The peak cylinder pressure was close to top dead center (TDC) for most of the baseline experiments (without RG blending). RG blending retarded the combustion timing toward a more optimized value, which led to higher indicated thermal efficiencies.

RG composition effects. Two similar cases of RG 75/25 and RG 50/50 were chosen for comparison. The EGR rates for the two cases were $(52.3 \pm 1.8)\%$ and $(51.7 \pm 1.0)\%$, respectively. Figure 12 shows pairs of constant λ and RG blend fraction for two cases of RG 75/25 and RG 50/50. While λ was identical in each pair, differences in the initial conditions and EGR rates led to small differences in the IMEP.

Fig. 10 Effect of RG on indicated mean effective pressure for operating points indicated in Fig. 3, error bars indicate ±2σ

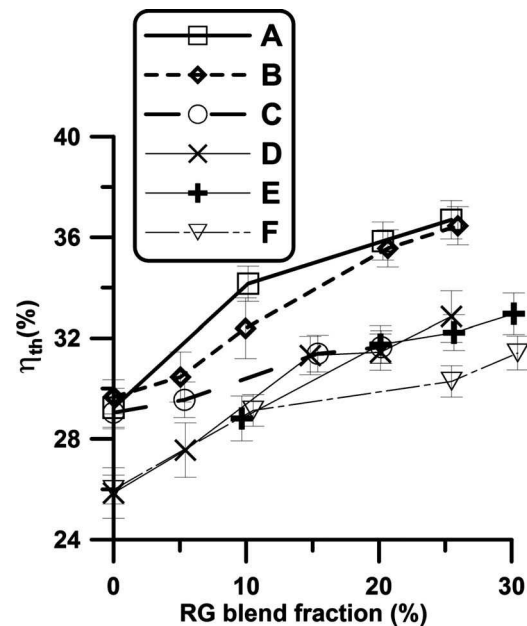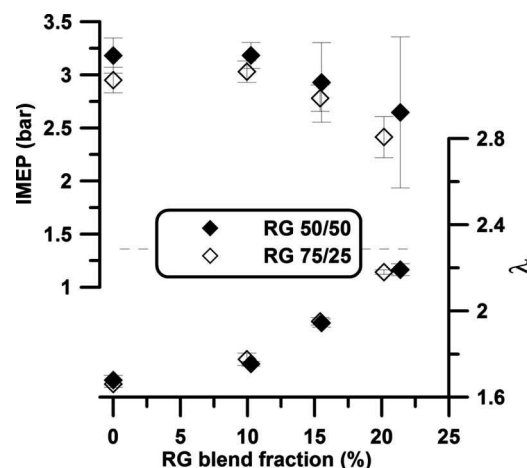**Fig. 12 Selected pairs of constant λ, similar EGRs, and identical RG blending fractions**

Journal of Engineering for Gas Turbines and Power
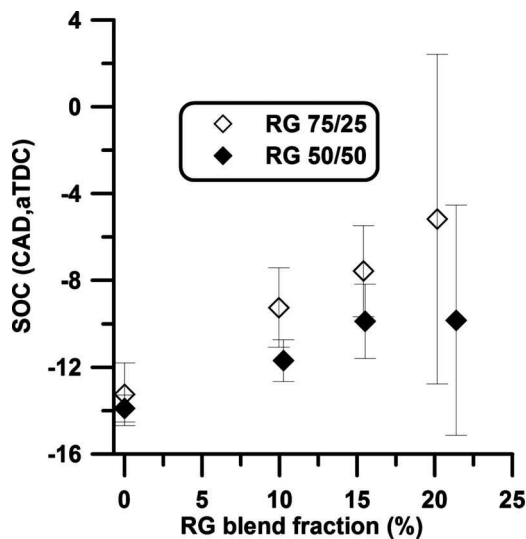
Fig. 13 Effect of RG composition on *n*-heptane HCCI combustion timing retardation, error bars indicate ±2σ

Fig. 15 Comparison of experimental pressure traces of point 1, data set F with ChemComb-SZM, experiment: supercharged *n*-heptane HCCI combustion, $N=800$ rpm, CR=11.8, $T_{intake,mix}=110°C$, intake pressure=143 kPa, $\lambda=2.94$, EGR=19.9%, and RG blend fraction=0.0%

Note that by increasing RG blend fraction, λ is also increased due to difficulties in finding constant λ cases within the operating range.

Figure 13 shows the effect of RG composition on retardation of *n*-heptane HCCI combustion phasing. Despite identical λ values, Fig. 13 shows that RG 75/25 was more effective in retarding the SOC than RG 50/50. At RG blend fraction=0%, the two operating points were virtually the same and the starts of combustion were identical. At RG blend fraction=10%, the difference between SOCs were 2.4 CAD. At RG blend fraction=15%, the difference between SOCs was 2.6 CAD, and at RG blend fraction=20% the difference in SOCs increased to 4.8 CAD.

Figure 14 shows the effect of RG composition on net rate of heat release for two cases of RG 75/25 (top) and RG 50/50 (bot-
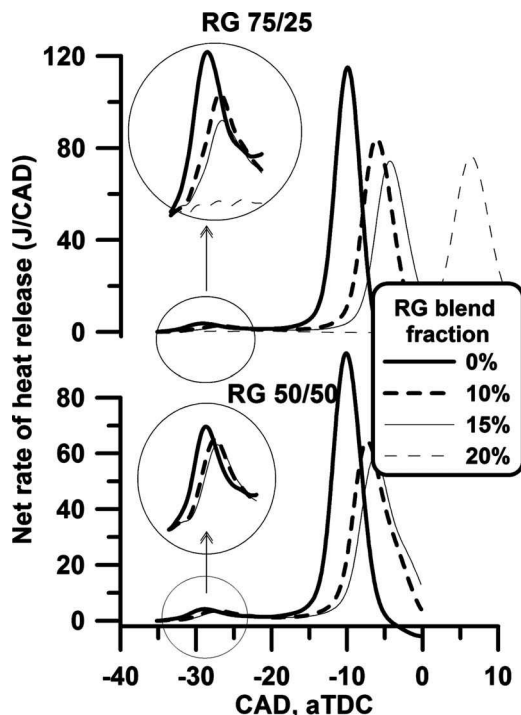
tom). As indicated, RG 75/25 was more effective at reducing low temperature heat release than RG 50/50 and the retardation of the high temperature heat release (HTHR) stage was larger in the RG 75/25 case.

7 Numerical Simulation

Model description. A MATLAB®-based stand alone thermodynamic model with detailed chemical kinetics was developed to investigate RG effects on HCCI combustion of *n*-heptane. The model, described previously by Kongsereeparp and Checkel [20–23], simulates the closed portion of an HCCI combustion cycle using a single-zone model (SZM) or multizone model (MZM) configuration. The initial conditions are prescribed pressure, temperature, and equivalence ratio (φ) at intake valve closure, or mass flow rates of the intake mixture components.

ChemComb-SZM was used in this study to simulate the thermodynamics and detailed chemical kinetics of the combustion process up until the point of ignition. This model was found to predict the SOC to within the range of the measured engine cyclic variations. Since ChemComb-SZM assumes homogeneity of temperature, residuals, and φ, it overpredicts P_{max}, $(dP/d\theta)_{max}$, IMEP, and other engine parameters. However, ChemComb-SZM proved to be computationally efficient and reasonably accurate for predicting the early stages of combustion. The *n*-heptane chemical kinetic mechanism used for this study was adopted from a semireduced chemical kinetic mechanism developed by Golovichev [24] with 57 species and 290 reactions.

Chemical kinetic model validation. Experimental data set F was chosen for the purposes of validating the numerical simulation. Cylinder pressure traces predicted by ChemComb-SZM were compared with the corresponding experimental data at the start of HTHR, which occurs just prior to the 10% cumulative heat release location (SOC). For each operating point, 100 consecutive cycles of cylinder pressure data were processed, and the cycles with maximum P_{max}, minimum P_{max}, and median P_{max} were plotted. For simplicity, these cycles were named P_{max} (maximum P_{max}), P_{min} (minimum P_{max}), and P_{median} (median P_{max}).

Figures 15 and 16 compare ChemComb-SZM predictions with experimental data for RG fractions of 0% and 30.4%, respectively. The complete validation results can be found in Ref. [25]. Figure 17 shows that the numerical simulation correctly predicts the trend of increasingly retarded SOC as the RG fraction increases.

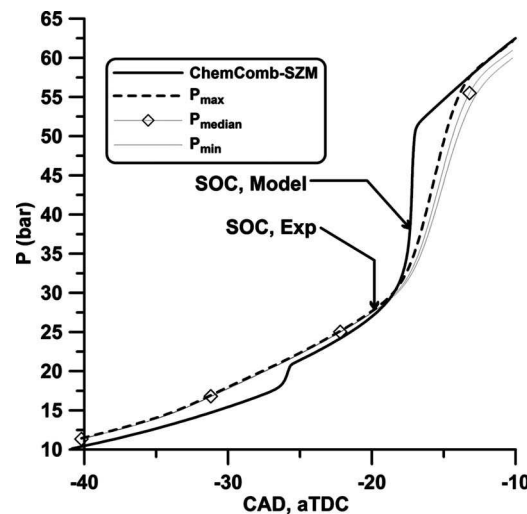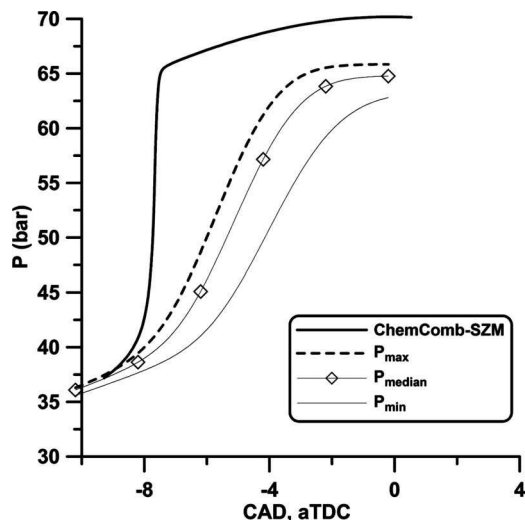**Fig. 14 Effect of RG composition on net rate of heat release**

Fig. 16 Comparison of experimental pressure traces of point 1, data set F with ChemComb-SZM, experiment: supercharged *n*-heptane HCCI combustion, $N=800$ rpm, CR=11.8, $T_{intake,mix}=110°$C, intake pressure=143 kPa, $\lambda=3.00$, EGR=21.7%, and RG blend fraction=30.4%

The experimental results showed that 10% RG blend fraction increased retarded SOC by 4.4 CAD, whereas ChemComb-SZM predicted 3.1 CAD of SOC retardation for 10% RG blending.

The differences between the numerical simulation and experimental data were reasonable given the assumptions inherent in the single-zone model and the experimentally observed cyclic variability in the SOC.

Detailed analysis using ChemComb-SZM. Figure 18 shows the cylinder temperature traces predicted by ChemComb-SZM for the experimental data set F in Fig. 3.

The cylinder temperature history during the early stages of low temperature heat release (-30 to -20 CAD) has been magnified in the figure. The compression temperatures of the high RG blend fraction blends were higher than those of the low RG blend fraction blends before low temperature heat release is initiated. After

Fig. 18 ChemComb-SZM simulation results for in-cylinder temperature during and after compression for data set F in Fig. 3

low temperature combustion starts, however, the trend reverses with lower temperatures predicted as the RG blend fraction increases.

The low temperature heat release behavior may be further investigated by looking at key species concentrations during the LTHR and NTC combustion stages. Figure 19 shows the mole fraction evolution of key intermediate radicals formed during the combustion process: hydrogen peroxide (H_2O_2), formaldehyde (CH_2O), and hydroxyl (OH). Both formaldehyde and hydrogen peroxide are key radicals that accompany two-stage auto-ignition behavior.

The radical pool formation is initiated during the LTHR stage and continues during the NTC delay period. Before the main combustion stage (HTHR), all intermediate species are converted to hydroxyl radicals.
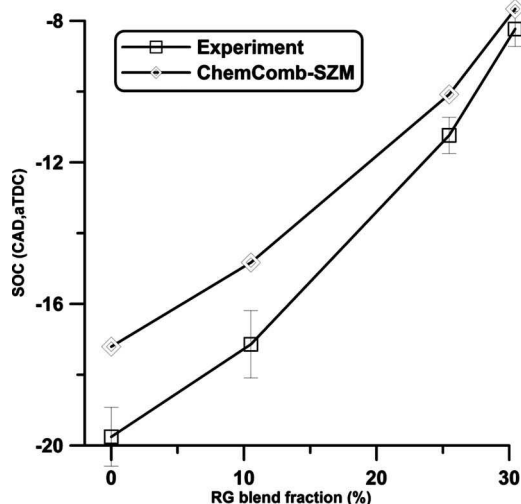

Fig. 17 A comparison of combustion timing (SOC) prediction by ChemComb-SZM with actual experimental combustion timing for data set F in Fig. 3, error bars on experimental SOC show the cyclic variation indicating $\pm 2\sigma$
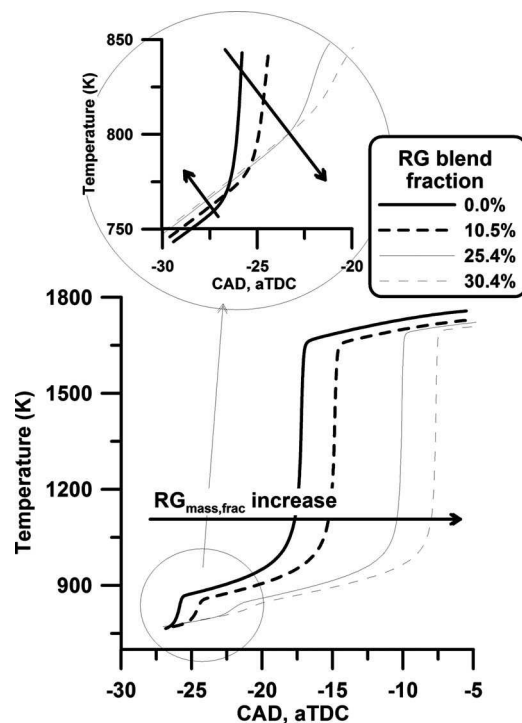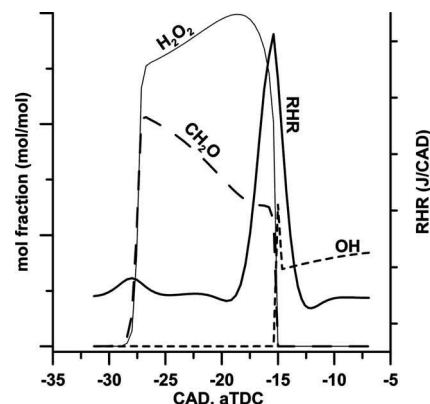

Fig. 19 Typical mole fraction traces of key species of OH, H_2O_2, and CH_2O compared with net rate of heat release in *n*-heptane HCCI combustion
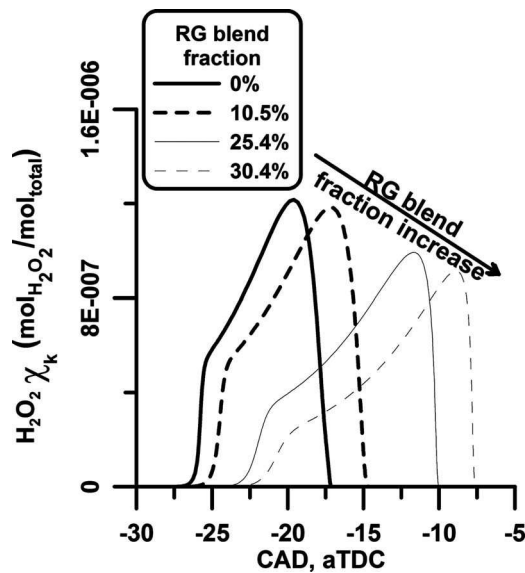
Fig. 20 Effect of RG on mole fraction of hydrogen peroxide (H_2O_2), *n*-heptane HCCI combustion simulated by ChemComb-SZM for data set F in Fig. 3

Fig. 21 Effect of RG on the reaction rates of H_2O_2, (*a*) production rate for Reaction 122, (*b*) production rate for Reaction 123, and (*c*) total production rate (from all 19 reactions)

The last stage is decomposition of the fuel molecules by OH radicals, which is associated with nonreversible reactions and abrupt heat release of the HTHR stage. Figure 20 shows the effect of RG on the H_2O_2 mole fraction. Increasing RG blend fraction decreased the molar fraction of H_2O_2 and retarded the timing of radical production.

Analysis of reaction rates in the main mechanisms used in ChemComb-SZM [24] indicates that Reaction 122 is the main source of H_2O_2 production during NTC

$$\text{Reaction 122:} \quad 2HO_2 \leftrightarrow O_2 + H_2O_2$$

Reaction 123 is the key reaction responsible for H_2O_2 destruction

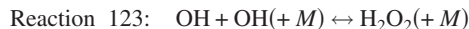$$\text{Reaction 123:} \quad OH + OH(+M) \leftrightarrow H_2O_2(+M)$$

Figure 21 shows that increasing the RG blend fraction increased both the production and destruction rates of the H_2O_2 radical during LTHR.

Figure 21(*c*) shows that increasing the RG blend fraction caused an overall net destruction of H_2O_2 radicals. The alteration of the key reaction rates happened during LTHR. Looking at the LTHR stage, the concentration of H_2O_2 radicals was decreased, as shown in Fig. 20. The mole fraction ratio of maximum OH to maximum H_2O_2 was decreased considerably. This ratio shifted progressively from $[OH]=0.94[H_2O_2]$ to $[OH]=0.08[H_2O_2]$, as the RG blend fraction increased from 0% to 30%, as shown in Fig. 22.

During LTHR, RG replaced most of the OH with H_2O_2 radicals through the following series of reactions:

$$\text{Reaction 101:} \quad H_2 + OH \leftrightarrow H_2O + H$$

$$\text{Reaction 97:} \quad CO + OH \leftrightarrow CO_2 + H$$

The H radical produced combines quickly with O_2 to form HO_2, and then with another H atom to form H_2O_2. OH is a highly active radical at low temperatures, while both HO_2 and H_2O_2 are almost inert during LTHR. Converting highly reactive OH radicals to less reactive HO_2 and H_2O_2 resulted in less chain branching reactions during LTHR, thus leading to less heat release during NTC and retardation of HTHR. These results are in agreement with findings of previous modeling and chemical kinetic studies such as Refs. [26,27].
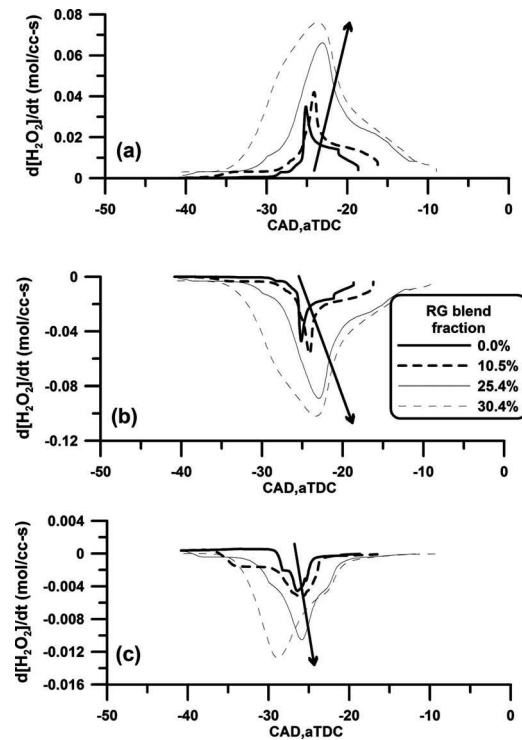
Figure 23 compares the SOC prediction of the numerical simulation to the experimental data for the two cases of RG 75/25 and RG 50/50.

ChemComb-SZM was able to predict the SOC to within the cyclic variability of the observed SOC for both cases. For the case of RG 50/50, the experimental results showed 2.4 CAD retardation in combustion timing with 10% RG compared with a prediction of 1.7 CAD in SOC retardation by ChemComb-SZM. For the case of RG 75/25, the experimental results showed 5.5 CAD in SOC retardation for a 10% RG blend fraction increase, while the numerical simulation predicted 5.1 CAD in combustion timing retardation.

Figure 24 shows the mole fraction of hydrogen peroxide as a function of crank angle for different RG blend fractions and RG

Fig. 22 Effect of RG on the ratio of maximum mole fraction during LTHR for OH/H_2O_2 ratio

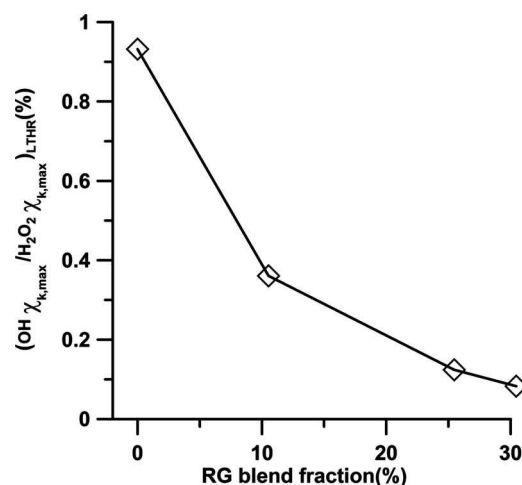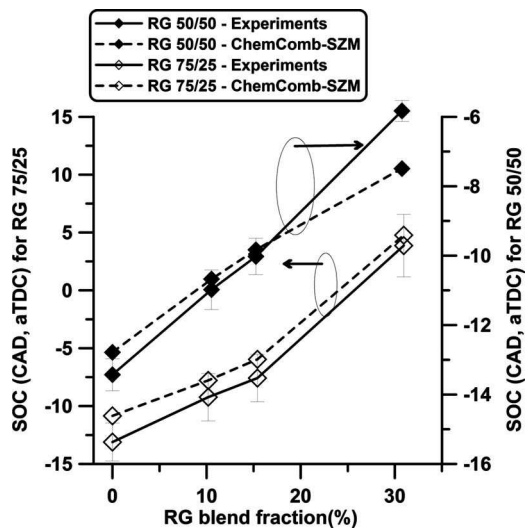**Fig. 23 A comparison of SOC prediction by ChemComb-SZM and experimental results for two cases of RG 75/25 (left Y-axis) and RG 50/50 (right Y-axis), error bars indicate ±2σ**

compositions of 75/25 and 50/50. The graphs show that increasing RG blend fraction for both RG compositions reduces the mole fraction of intermediate radicals such as H_2O_2.

There was less delay in the formation of the H_2O_2 intermediate radical for the case of RG 50/50. Based on H_2O_2 radical concentrations shown in Fig. 24, the timing of maximum H_2O_2 molar concentration was retarded by 5 CAD for RG 75/25 and less than 3 CAD for RG 50/50. Thus, the RG 75/25 composition that contains a higher concentration of hydrogen gas is more effective in retarding the combustion timing.

8 Discussion

HCCI combustion timing is a complex function of several engine operating parameters such as compression ratio, intake temperature, EGR, air/fuel ratio, speed, and intake pressure. In this study, the effect of RG blending fraction and composition on *n*-heptane HCCI combustion timing was investigated, keeping

other influential parameters constant. It was found that RG blending was effective in retarding *n*-heptane HCCI combustion over a wide range of conditions.

In the *n*-heptane experiments presented in this paper, λ did not have a large influence on HCCI combustion timing. In Fig. 5, λ variation between selected groups of operating points (Fig. 3) did not significantly change the SOC. EGR altered *n*-heptane HCCI combustion timing in distinct steps, as indicated in Fig. 5. On the other hand, an increase in EGR from 30% to 50% retarded combustion timing by an average of 5 CAD independent of λ. These results are comparable to those obtained by Peng et al. [28], in which a high compression ratio (CR=18.0) was used to operate a HCCI combustion engine with *n*-heptane. The engine was operated with an extremely lean (6.0<λ<14.0 at 0% EGR) and highly diluted mixture (up to 70% EGR) with intake temperature=30°C. The timings of the LTHR and HTHR combustion phases were strong functions of EGR and independent of λ. λ only affected HTHR timing when λ>9.0. In the current study, λ reduced LTHR_max, prolonged NTC, and delayed HTHR_max,time (see Fig. 7–9).

Whereas λ did not have a strong influence on *n*-heptane HCCI combustion timing and EGR effects came with an IMEP penalty, RG was shown to be capable of combustion timing control with power and fuel conversion efficiency gains. For the selected cases, the indicated power (IMEP) was increased by an average of 0.25 bar for each 10% RG blend fraction increase (see Fig. 10), and indicated that thermal efficiency was increased by an average of 2.8% for a 10% RG blend fraction increase (see Fig. 11). Note that the efficiency penalty of fuel reforming was not considered in the indicated thermal efficiency calculation. If a 78% reforming efficiency is assumed for partial oxidation reforming of a hydrocarbon fuel (see Ref. [29]), and replacing 10% of *n*-heptane with RG, a total cycle efficiency decrease of less than 1% is expected for RG blend fraction=10%, which would be compensated by a 2.8% increase in indicated thermal efficiency due to RG blending. Increasing indicated power and indicated thermal efficiency was the result of more optimized combustion timing by RG blending.

A single-zone thermodynamic model with detailed chemical kinetics was used to interpret the experimental data. The numerical simulation SOC predictions showed good agreement with the experimental data, and qualitatively predicted the SOC retardation due to RG blending (see Fig. 17). During the compression stroke, the numerical simulation predicted higher temperatures as the RG
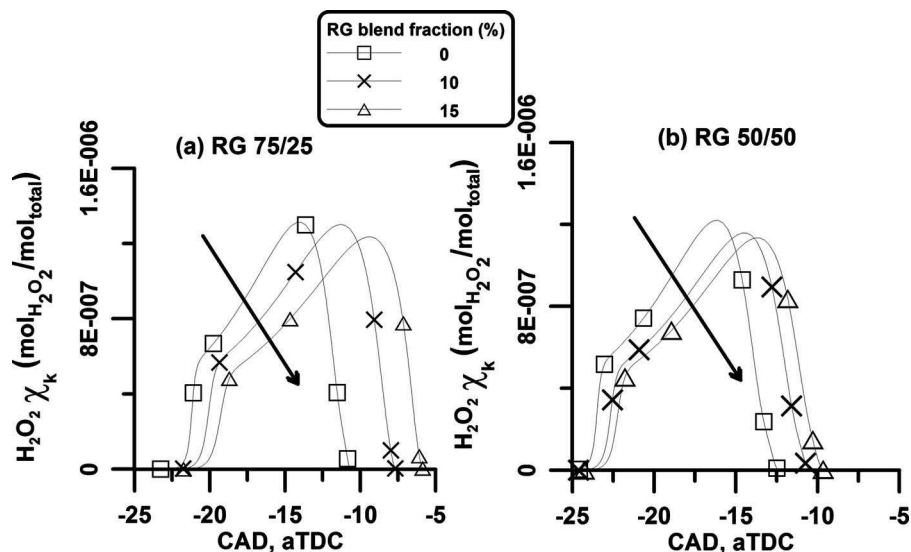

Fig. 24 Effect of RG composition on H_2O_2 mole fraction for (a) RG 75/25 and (b) RG 50/50

blend fraction increased (see Fig. 18). Replacing *n*-heptane (specific heat of $C_p = 224.9$ J/mol K [30]) with RG (specific heats of $C_{p,H_2} = 28.84$ J/mol K and $C_{p,CO} = 29.14$ J/mol K [30]) led to higher compression temperatures. When the low temperature reactions were initiated around 760 K, the higher RG blending fractions produced lower temperatures after LTHR and during the NTC delay period. This is an indication of lower heat release during LTHR by the higher RG blend fractions that confirmed the experimental observations.

Lower heat release during LTHR was associated with a lower molar concentration of intermediate radicals as the RG blend fraction increased. For example, increasing the RG blend fraction decreased the molar concentration of H_2O_2 during NTC (see Fig. 20). However, lower H_2O_2 molar concentrations during the NTC delay period were not a result of low reaction rates. In the chemical kinetics mechanism that was used in this study, 19 reactions contributed to the production and destruction of H_2O_2. Among them, Reactions 122 and 123 were the main H_2O_2 production and destruction reactions, respectively. Increasing the RG blend fraction increased the rates for Reactions 122 and 123 (see Figs. 21(*a*) and 21(*b*)). However, the summation of all 19 reaction rates showed a relative increase in the H_2O_2 radical destruction rate. Increasing the RG blend fraction increased both the production and destruction of H_2O_2 radicals, but the net effect was in favor of lowering the H_2O_2 molar concentration (see Fig. 21(*c*)). The effect of RG blending was to progressively convert highly reactive hydroxyl radicals formed during LTHR to less reactive H_2O_2 radicals (see Fig. 22).

In practice, the H_2 to CO ratio in RG varies depending on the hydrocarbon fuel, the reforming technique, and the fuel reforming conditions. To investigate effects of RG composition on SOC retardation of *n*-heptane HCCI combustion, two extreme cases of RG were used. It was found that both RG compositions of RG 75/25 and RG 50/50 were effective in retarding *n*-heptane HCCI combustion timing, but RG 75/25 was more effective (see Fig. 13). The experimental results showed that LTHR$_{max}$ reduction with RG 75/25 was stronger than with RG 50/50 (see Fig. 14). Numerical simulations were performed to confirm the RG composition effects, which were in agreement with the findings of Shudo and Yamada [27] and Shudo and Takahashi [31] for RG addition on HCCI combustion of DME. Increasing the H_2 fraction in RG also increased the combustion retardation in their study. The current results are also in agreement with the results of numerical simulations performed by Subramanian et al. [26]. Using both detailed and reduced chemical kinetic mechanisms, the authors concluded that at temperatures around 600 K, the presence of CO lengthens *n*-heptane HCCI ignition delay by 5–10%, while H_2 addition lengthens the ignition delay by 10–15%.

Both H_2 and CO suppress the formation of radical pools. In the chemical kinetic mechanism used, Reactions 97 and 101 are responsible for OH radical consumption by CO and H_2, respectively. Similar to the discussion in Ref. [27], Reaction 101 is 3–6 times faster than Reaction 97 in the temperature range of 700–1000 K, where low temperature oxidation occurs. Migrating from RG 75/25 to RG 50/50 favors Reaction 97, and radical consumption by RG was reduced. The similarity of combustion suppression by H_2 and CO makes the application of fuel reforming attractive as a mean of combustion timing control for fuels with two-stage combustion. Practically, it means that small variations in onboard fuel reformer output during its operation will not have a large effect on combustion timing control.

9 Conclusions

The effects of reformer gas blends (RG, binary mixture of H_2, and CO) on homogenous charge compression ignition combustion of *n*-heptane were examined. It was found that RG blending was effective in retarding the combustion phasing. The mechanisms were reduction in the low temperature heat release followed by prolongation of the negative temperature coefficient delay period and a delay in the high temperature heat release. On average, increasing RG blend fraction by 10% retarded combustion timing by 4.4 crank angle deg.

Shifting *n*-heptane HCCI combustion timing toward a more optimized value increased indicated power at constant energy flow rate, as well as indicated thermal efficiency. On average, increasing the RG blend fraction by 10%, increased IMEP by 0.25 bar and indicated thermal efficiency by 2.8%.

A single-zone chemical kinetics model confirmed the experimental observations. It was found that RG initially increased compression temperatures, but after the low temperature heat release stage it reduced in-cylinder temperatures by lowering the energy released during the low temperature reactions. The model also showed that RG blending enhanced both the production and destruction of intermediate radicals during low temperature reactions. The overall effect was to decrease the total concentration of intermediate radicals.

Two extreme cases of RG compositions with 75% H_2–25% CO (RG 75/25) and 50% H_2–50% CO (RG 50/50) were examined. It was found that both RG compositions retarded *n*-heptane HCCI combustion phasing, but the higher H_2 content RG was more effective in retarding the combustion phasing.

Nomenclature

ChemComb = thermodynamic model of HCCI combustion with detailed chemical kinetics

GHR = gross accumulative heat release (J)

HTHR = high temperature heat release (J)

LTHR = low temperature heat release (J)

NRHR = net rate of heat release (J/CAD)

RG = reformer gas (H_2/CO) mixture

SOC = start of combustion (CA10)

P_{max} = maximum cylinder pressure (bar)

$(dP/d\theta)_{max}$ = maximum rate of pressure rise (bar/CAD)

$T_{intake,mix}$ = intake mixture (air, fuel, RG, and EGR) temperature

σ = standard deviation of cyclic variation

References

[1] Upatniek, A., Mueller, C. J., and Martin, G. C., 2005, "The Influence of Charge-Gas Dilution and Temperature on DI Diesel Combustion Processes Using a Short-Ignition-Delay, Oxygenated Fuel," SAE Paper No. 2005-01-2088.

[2] Sjöberg, M., and Dec, J. E., 2003, "Combined Effects of Fuel-Type and Engine Speed on Intake Temperature Requirements and Completeness of Bulk-Gas Reactions for HCCI Combustion," SAE Paper No. 2003-01-3173.

[3] Christensen, M., Hultqvist, A., and Johansson, B., 1999, "Demonstrating the Multi-Fuel Capability of a Homogeneous Charge Compression Ignition Engine With Variable Compression Ratio," SAE Paper, 1999-01-3679.

[4] Stanglmaier, R. H., Ryan, T. W., and Souder, J. S., 2001, "HCCI Operation of a Dual-Fuel Natural Gas Engine for Improved Fuel Efficiency and Ultra-Low NOx Emissions at Low-to-Moderate Engine Loads," SAE Paper No. 2001-01-1897.

[5] Zheng, Z., Yao, M., Chen, Z., and Zhang, B., 2004, "Experimental Study on HCCI Combustion of Dimethyl Ether (DME)/Methanol Dual Fuel," SAE Paper No. 2004-01-2993.

[6] Jamal, Y., and Wyszynski, M. L., 1994, "On-Board Generation of Hydrogen-Rich Gaseous Fuels—A Review," Int. J. Hydrogen Energy, **19**(7), pp. 557–572.

[7] Dicks, A. L., 1996, "Hydrogen Generation From Natural Gas for the Fuel Cell Systems of Tomorrow," J. Power Sources, **61**, pp. 113–124.

[8] Shudo, T., 2006, "An HCCI Combustion Engine System Using On-Board Reformed Gases of Methanol With Waste Heat Recovery: Ignition Control by Hydrogen," Int. J. Veh. Des., **41**, pp. 206–225.

[9] Tsolakis, A., and Megaritis, A., 2005, "Partially Premixed Charge Compression Ignition Engine With On-Board H_2 Production by Exhaust Gas Fuel Reforming of Diesel and Biodiesel," Int. J. Hydrogen Energy, **30**, pp. 731–745.

[10] Eng, J. A., Leppard, W. R., and Sloane, T. M., 2002, "The Effect of POx on the Autoignition Chemistry of n-Heptane and Iso-Octane in an HCCI Engine," SAE Paper No. 2002-01-2861.
[11] Hosseini, V., and Checkel, M. D., 2006, "Using Reformer Gas to Enhance HCCI Combustion of CNG in a CFR Engine," SAE Paper No. 2006-01-3247.
[12] Hosseini, V., and Checkel, M. D., 2007, "Effect of Reformer Gas on HCCI Combustion—Part I: High Octane Fuels," SAE Paper No. 2007-01-0208.
[13] Hosseini, V., and Checkel, M. D., 2007, "Effect of Reformer Gas on HCCI Combustion—Part II: Low Octane Fuels," SAE Paper No. 2007-01-0206.
[14] Hosseini, V., and Checkel, M. D., 2005, "Alternative Mode Combustion Study: HCCI Fueled With Heptane and Spark Ignition Fueled With Reformer Gas," ASME Internal Combustion Engine Fall Technical Conference, Ottawa, Canada, Paper No. ICEF2005-1240.
[15] Mueller, C. J., 2005, "The Quantification of Mixture Stoichiometry When Fuel Molecules Contain Oxidizer Elements or Oxidizer Molecules Contain Fuel Elements," SAE Paper No. 2005-01-3705.
[16] Heywood, J. B., 1988, Internal Combustion Engine Fundamentals, McGraw-Hill, New York.
[17] Chang, J., Güralp, O., Filipi, Z., Assanis, D., Kuo, T.-W., Najt, P., and Rask, R., 2004, "New Heat Transfer Correlation for an HCCI Engine Derived From Measurements of Instantaneous Surface Heat Flux," SAE Paper No. 2004-01-2996.
[18] Hosseini, V., and Checkel, M. D., 2008, "Reformer Gas Composition Effect on HCCI Combustion of N-Heptane, Iso-Octane, and Natural Gas," SAE Paper No. 2008-01-0049.
[19] Hosseini, V., 2008, "Reformer Gas Application in HCCI Combustion Engine," Ph.D. thesis, University of Alberta, Edmonton, AB, Canada.
[20] Kongsereeparp, P., Kashani, B., and Checkel, M. D., 2005, "A Stand-Alone Multi-Zone Model for Combustion in HCCI Engines," ASME Internal Combustion Engine Fall Technical Conference, Ottawa, Canada, Paper No. ICEF2005-1241.
[21] Kongsereeparp, P., and Checkel, M. D., 2007, "Investigating the Effects of Reformed Fuel Blending in a Natural Gas- and N-Heptane-HCCI Engine Using a Multi-Zone Model," SAE Paper No. 2007-01-0205.
[22] Kongsereeparp, P., and Checkel, M. D., 2007, "Novel Method of Setting Initial Conditions for Multi-Zone HCCI Combustion Modeling," SAE Paper No. 2007-01-0674.
[23] Kongsereeparp, P., and Checkel, M. D., 2007, "Investigating the Effects of Reformed Fuel Blending in a Methane- or N-Heptane-HCCI Engine Using a Multi-Zone Model," SAE Paper No. 2007-01-0205.
[24] Golovichev, V., 2007, http://www.tfd.chalmers.se/~valeri/MECH.html.
[25] Hosseini, V., Neill, W. S., and Checkel, M. D., 2008, "Controlling N-Heptane HCCI Combustion With Partial Reforming: Experimental Results and Modeling Analysis," ASME Internal Combustion Engine Spring Technical Conference, Chicago, IL, Paper No. ICEF200-1618.
[26] Subramanian, G., Da Cruz, A. P., Bounaceur, R., and Vervisch, L., 2007, "Chemical Impact of CO and H2 Addition on the Auto-Ignition Delay of Homogenous N-Heptane/Air Mixtures," Combust. Sci. Technol., 179(9), pp. 1937–1962.
[27] Shudo, T., and Yamada, H., 2007, "Hydrogen as an Ignition-Controlling Agent for HCCI Combustion Engine by Suppressing the Low-Temperature Oxidation," Int. J. Hydrogen Energy, 32(14), pp. 3066–3072.
[28] Peng, Z., Zhao, H., and Ladommatos, N., 2003, "Effects of Air/Fuel Ratios and EGR Rates on HCCI Combustion of N-Heptane, a Diesel Type Fuel," SAE Paper No. 2003-01-0747.
[29] Docter, A., and Lamm, A., 1999, "Gasoline Fuel Cell Systems," J. Power Sources, 84, pp. 194–200.
[30] Dean, J. A., 1999, Lange's Handbook of Chemistry, 15th ed., McGraw-Hill, New York.
[31] Shudo, T., and Takahashi, T., 2004, "Influence of Reformed Gas Composition on HCCI Combustion of Onboard Methanol-Reformed Gases," SAE Paper No. 2004-01-1908.